



Research article

Mechanistic analysis of matrix-acid treatment of carbonate formations: An experimental core flooding study

Saber Mohammadi ^{a,b,*}^a Petroleum Engineering Department, Research Institute of Petroleum Industry (RIPI), Tehran, Iran^b Petroleum Engineering Department, Amirkabir University of Technology (Tehran Polytechnique), Tehran, Iran

ARTICLE INFO

Keywords:

Acid injection
Wormholes
Carbonate rock
Optimum injection rate

ABSTRACT

Despite the extensive works carried out on optimal design of the acidizing operations, the detailed mechanisms of the wormholes formation and propagation within the rock structure and their effects on optimum acid injection rate have not been well studied in the available literature. In this work, high pressure-high temperature (HP-HT) acid injection experiments and computed tomography (CT) scan imaging were performed by HCl 15 wt% to discover the mechanisms underlie the creation of wormholes and their extension in the carbonate rocks. The pressure drop profiles and permeability variations before and after acidizing process were employed to identify the optimum acid injection rate. As a final point, core effluent samples were collected and analyzed for justification of the HP-HT experimental results. For performed HP-HT experiments, acid injection rate of 7 cm³/min was obtained as the optimal acid injection rate. The maximum permeability improvement, $K_f/K_i = 11.2$, was achieved at the optimum acid injection rate corresponded to the minimum acid breakthrough volume, as well as the acid consumption. The results obtained from the CT scan analysis show that the wormhole created in core C.4 is close to the optimal conditions with a single distinctive wormhole to bypass the damage. At acid injection rates lower or higher than the optimum injection rate, the shape of the wormholes changes to conical at very low injection rates and ramified at high injection rates. The highest concentration of calcium at effluent samples was observed for the minimum and maximum injection rates (1 and 15 cm³/min), respectively. The maximum contact time and highest contact area between the acid and rock were attained at minimum and maximum acid injection rates, respectively. As this work was performed at realistic oilfield conditions, it can be used for effective plan, execution and optimization of the acidizing operation in carbonate reservoirs.

1. Introduction

Acidizing treatments are commonly used to remove near-wellbore damage, create artificial flow channels and improve impressively the well productivity [1]. Acid treatment strategy is categorized in three different ways including wellbore cleaning (or acid washing), acid fracturing and matrix acidizing [2–4]. An acid washing scenario is designed to clean the tubular and wellbore as well as to remove the scales (e.g. calcium carbonate), rust, and other debris from the perforations and well-completion components [5,6]. The acid can be placed into the wellbore at a desired position and allowed to react with the scale, or it is circulated back and forth across the

* Petroleum Engineering Department, Research Institute of Petroleum Industry (RIPI), Tehran, Iran.
E-mail addresses: mohammadi.sab@gmail.com, mohammadisab@ripi.ir.

<https://doi.org/10.1016/j.heliyon.2024.e24936>

Received 20 September 2023; Received in revised form 3 January 2024; Accepted 17 January 2024

Available online 23 January 2024

2405-8440/© 2024 The Author. Published by Elsevier Ltd. This is an open access article under the CC BY-NC-ND license (<http://creativecommons.org/licenses/by-nc-nd/4.0/>).

casing perforation or formation face, without penetrating into the formation near the wellbore [7,8]. In acid fracturing process, acid is injected into the formation above the hydraulic pressure to break the formation and create new flow channels or open existing fractures [9–11]. Stimulation technique is important as long as the produced highly permeable fracture paths remain open after the acidizing operation. The main purpose of this technique is to create flow paths into the undamaged portions of the reservoir formation and thus increase the drainage surface area into the wellbore [5]. Acid fracturing is confined to the carbonate reservoirs and is not used to stimulate the sandstones, shale, or coal-seam reservoirs [12–14]. The aim of matrix acidizing is to improve the oil production by dissolving formation damage or creating the new pathways within several inches to a foot or two around the borehole [15,16]. It is also used to develop the wormhole network and to evade any induced damage prompted by treatment fluid and pre-flush/post-flush fluids [17,18]. Acid is injected into the well penetrating the rock pores at pressures below the fracture pressure. This is the main difference between the acid fracturing and matrix acidization [19]. Injection rates resulting in pressures below the fracture pressure are termed "matrix acidizing" while in fracturing process the applied pressure is above the fracture pressure which is termed as "acid fracturing" [19,20]. In matrix acidizing, a deep penetration of the wormholes around the well is required; in the acid-fracturing process, fluid leak-off must be limited and wormholes are prohibited. Detailed laboratory tests are essential to improve the design of these operations [20–23].

At present, the world demand for energy is growing and predicted and certainly more energy will be required in the near future [24, 25]. To attain this demand, high temperature reservoir acidizing is of paramount importance because most of the oil and gas reserves are located in deep structures with high temperature condition [25,26]. Acidizing may, in fact, be the oldest stimulation technique and still in modern use. Still, many researchers and industrial companies are developing different acid systems to be used at different operational conditions of pressure and temperature [27]. Acidizing can be used in preference to hydraulic fracturing technique in many situations such as naturally fractured reservoirs, formations with high permeability and loose packing, and eliminating formation damage around the wellbore [25,28]. Furthermore, acidizing can be applied in the depleted sandstone reservoirs wherever the hydraulic fracturing cannot be executed.

Mixtures of hydrofluoric acid (HF) and hydrogen fluoride acid (HF) have been the most usual acidizing treatment for dissolving the minerals that cause damage [29,30]. These treatments are preceded by a pre-flush of either HCl varying between 7 % and 15 % or weaker acids such acetic acid (CH_3COOH) to dissolve the carbonates and evade precipitation of the calcium fluoride. The main HCl-soluble minerals are calcite, dolomite, and siderite which also do not produce precipitates [31]. It is critical to optimize the acidizing fluid and conditions for the success of a matrix treatment. The acidizing operation may be failed if the proper additives in a compatible medium are not used [16]. The aim of designing acidizing fluid is for elimination of or escaping from the induced damage, whereas additives are used to inhibit excessive corrosion, prevent formation of the asphaltene and stick sludge or emulsion, avoid iron precipitation, improve the coverage of the acidized zone and avoid precipitation of the reaction products [32,33]. For efficient

Table 1
Summary of the main works reported in the literature.

Authors	Year	Fluid Type	Rock Type	Main Results
Daccord et al. [97]	1993	Describing the flow properties of wormholes by a quantitative model		<ul style="list-style-type: none"> In damaged and undamaged primary porosity carbonates: flow will take place in natural porosity. In undamaged double porosity and damaged and undamaged secondary porosity formations: flow takes place in fractures. For damaged double porosity carbonates, flow takes place in native porosity, since damage is mostly located in secondary porosity.
Bazin et al. [98]	1995	HCl	Limestone	Development of a methodology by the experimental measurement of acid propagation rates and distances.
Ziauddin and Bize [99]	2007	15 wt% HCl	Carbonate	Similar porosity spatial distributions (PSD) exhibit similar trends in pore-volume to breakthroughs (PVBT).
Talbot and Gdanski [100]	2008	HCl		<ul style="list-style-type: none"> Development of a global model to describe carbonate matrix acidizing by hydrochloric acid. The wormhole efficiency does not seem to be a function of temperature but does appear to be strongly affected by the acid concentration.
Al-Ghamdi et al. [51]	2014	Regular and VES-based acids	Calcite rock	Critical rate = $3 \text{ cm}^3/\text{min}$; For permeability ratios >10 , careful design of acid-placement treatment.
Ortega and Nasr-El-Din [39]	2014	10 wt% Methanesulfonic acid (MSA)	Indiana limestone	<ul style="list-style-type: none"> At low injection rate: face dissolution and conical channels. At high injection rate: ramified wormhole.
Qi et al. [42]	2017	36–38 wt% Hydrochloric acid	artificial carbonate core	<ul style="list-style-type: none"> At low injection rate: face dissolution. At high injection rate: uniform dissolution.
Sidaoui et al. [53]	2018	HCl	Carbonate	Simulation: Prediction of optimum injection rate.
Guo et al. [13,49]	2020a, b	20 %HCl 20 %HCl+5 %VES	Fractured carbonate	<ul style="list-style-type: none"> Fracture width $<50 \mu\text{m}$: acidizing has poor effect. Fracture width = $50 \mu\text{m}$–$200 \mu\text{m}$: better acidizing effect, and the fracture permeability recovery rate reaches. 100 %–400 %. Fracture width $>200 \mu\text{m}$: acidizing has poorer effect since etching patterns of the surface changed from groove-like etching into uniform etching.
Sayed et al. [54]	2023	28 wt% HCl	Dolomite-rich formations	Proposed 3 formulations to accelerate the reaction rate by up to 30 % compared to using 28 wt% HCl without the additives.
Ahmadi et al. [55]	2023	Simulation by: Association rule mining (ARM)		Operational decisions by assisting in the design of due stimulation jobs.
Jia et al. [56]	2023	Modeling by: Finite volume method &		Development of a rheology model to describe the different viscosity constitutive relationships of acid fluids.

performance of acidizing additives in the package, fluid medium conditions should be carefully designed [26,34]. The failure rate of acidizing operation has been reported to be in the range of 25–32 % [25,35,36]. The reasons of operation failure are poor candidate selection, lack of mineralogical and fluid information, unsuitable chemical selection, not considering pressure and temperature conditions of operation in acidizing package design, lack of diversion plans, etc. [1,37].

The success of an acidizing treatment in detrital carbonate reservoirs is approved by development of continuous wormholes within the rock structure [38]. Wormholes are deep, highly branched dissolution channels made by the reaction of acid with carbonate rocks. The diameter of these ramified channels are an order of magnitude larger than the natural pores of the rock [38]. It has been progressively found that the breakthrough volume of the injected acid is certainly related to the optimal acid injection rate. The optimum acid injection rate is corresponded to the minimum acid volume for breakthrough of the generated wormholes [39–43]. The optimum acid injection rate is a complicated function of the pressure, temperature, acid dosage, permeability of the porous rock, size-distribution of the pores and throats, and its composition which should be taken into account during the acidizing procedures [20, 39,44,45]. Accordingly, evaluation and characterization of the wormholes and their creation mechanisms are of critical importance for effectual design of an acidizing operation. Optimization of the aforementioned parameters maximizes the efficiency of acidizing job and therefore results in prolonged well production and high oil recovery factor [46–50]. Over the last decades, extensive experimental and theoretical investigations have been paid for calculation of the optimum acid injection rate in carbonate formations. Complete reviewing of the literature works is out of scope of this paper and can be found in related references [39,42,49–57]. Moreover, the main results of researches by others have been summarized in Table 1.

In spite of the extensive works by many researchers in matrix acidizing area, the wormholes propagation, main mechanisms of the wormholes extension and the effects of different operational parameters on optimum acid injection rate have not been comprehensively assessed. In addition, most of the reported works in the literature have been performed at ambient conditions. The findings and conclusions drawn from the laboratory studies at ambient conditions cannot be essentially applied to high pressure-high temperature (HP-HT) environments (i.e. operational conditions). In this study, HP-HT acidizing injection experiments were conducted to analyze and describe the mechanisms involved in wormhole formation and propagation in the carbonate rock samples. Acidizing fluid package used in the injection experiments was optimized by the static experiments. The pressure drop data in terms of the injected pore volume of acid and variations in permeability at initial and final states, all through the HP-HT injection experiments, were employed to determine the optimum acid injection rate during the propagation of the wormholes. Development of the wormholes within the core samples were visualized by CT scan technique, and the mechanisms underlie the propagation of the wormholes were discussed in detail. Finally, the core effluent samples were analyzed for calcium ion concentration (Ca^{+2}) and medium alkalinity. Therefore, our study aims to fill the gap in the literature regarding the mechanisms responsible for acid stimulation process in matrix of the reservoir cores.

2. Experimental section

In this work, the experiments have been executed in three main parts: (1) preparation of the core samples, (2) measurement of the petrophysical properties of the core and characteristics of injection fluids, (3) fluid injection tests. Following experimental procedures have been established to achieve the purposes of this work.

2.1. Preparation of core samples

Core samples are cut in the desired dimensions to be appropriately used in the flooding setup. After preparing the core samples in terms of specific length and diameter, they are washed with organic solvents in order to remove organic and/or inorganic substances from their porous spaces to calculate the actual volume of the core samples [39]. The core samples are soaked in hot petroleum solvent (toluene) to wash the core samples and expel the hydrocarbons and possible water or drilling fluid from the inside of them [58,59]. After the hydrocarbon and water are dissolved in the solvent, the core samples are washed by the Soxhlet Extractor assembly. The washed core samples, which are free from any hydrocarbons and drilling fluid, are placed inside the oven until the solvent inside and on its surface evaporates and dries completely. It should be emphasized that the hot solvent used to remove any contaminants from the hydrocarbon of the core sample should not react with the rock or causes damage by the minerals. The typical effective solvents include toluene, methanol, xylene, chloroform or azeotropic [60].

Table 2
General characteristics of the core samples used in this study.

Core No.	Weight (gr)	Length (cm)	Diameter (cm)	Porosity (%)	Permeability (md)	Density (g/cm^3)
C.1	253.9	9.99	3.81	14.66	3.076	2.700
C.2	360.8	10.14	3.82	13.37	2.320	2.701
C.3	233.7	9.43	3.83	20.01	4.918	2.697
C.4	247.9	9.49	3.83	15.89	5.011	2.698
C.5	238.7	9.43	3.83	18.51	8.105	2.701

2.2. Characteristics of core samples and injection fluids

2.2.1. Characterization of core samples

All core samples are selected from a carbonate formation in an oilfield located in south west of Iran. The cores were extracted through a sampling procedure by coring tools (i.e. long metal cylinders) [61,62]. The coring procedure was performed in pay zone at depth of 3827 m. The composition of the core samples were determined through the X-ray powder diffraction (XRD) analysis, model PANalytical X'Pert PRO ($\lambda = 0.15406$ nm) [63,64]. The general characteristics of the core samples, determined by petrophysics and flow tests, and their images are given in Table 2 and Fig. 1. In addition, the composition of the core samples are given Table 3. The core samples were mainly composed of Calcite (CaCO_3) and Dolomite ($\text{CaMg}(\text{CO}_3)_2$).

2.2.2. Characterization of injected fluids

For flooding experiments, appropriate acidizing package(s) should be determined. For simulation of the oilfield conditions, acid package with specific concentration and proper additives should be designed. Based on previous studies on this reservoir, HCl (15 wt %) was used for preparation of the acidizing package. Typically, HCl concentration ranging from 5 to 28 wt% may be used in either continuous or a batch mixing system [65,66]. Based on the rock, fluid and well structure, different additives with specified concentrations were used in the acidizing package. The formulation of the designed acidizing package is given in Table 4. Performance of all additives have been investigated through the standard benchmarks quality control (QC) procedures [32,67,68]. The performance of each additive was tested in the presence of other additives considering the chemical and physical properties of additives, and their interactions within the fluid medium. The proposed acidizing package was determined by the benchmark QC experiments among the 10 possible formulations. After performing all the experiments and analyzing the results, optimal formula was selected as the most efficient package used in this work. Fig. 2 depicts the images of the designed optimum acidizing package. As seen in the images, the proposed package is completely homogeneous and all the additives are compatible with no deposit or phase-separation from the fluid medium. A full description of the mechanism of different additives and their performance tests aren't the subject of this paper. More information can be extensively found in the literature. The brine injection scenarios are performed in different sections to simulate the reservoir saturation state. The core samples were vacuumed, and then they were saturated with synthetic brine equivalent to the formation water composition of the reservoir considered in this study. Brine specifications are given in Table 5. The brine composition is comparable with composition of the formation water in other studies [69,70].

2.3. Fluid injection setup and tests

In this section, flooding experiments have been conducted to simulate the dynamic and static formation damage on the core samples. The flow diagram of the core flooding experiment and photograph of the flooding assembly are shown in Figs. 3 and 4. The core flooding system is composed of a modified Hassler type core-holder with four fluid chambers which two of them are acid resistant, a differential pressure transducer to measure the pressure drop across the core sample, a back pressure regulator, a Vinci pump for injection of the fluid and a pneumatic pump (Alemite 7783-C4 oil pump) to exert the overburden pressure, a collector in the exit point of the cores for collection of the produced fluid, and a computer equipped with specific in-house software for data recording. Hassler core-holders use a Viton™ or buna-N rubber membrane, to provide a barrier between the confining fluid (i.e. oil or water) and the core sample. The designed core-holder holds the core samples up to 12.0 cm in length and 5.0 cm in diameter. The maximum working pressure and temperature of the core-holder is 8.274×10^4 kPa and 150°C . Two of the fluid chambers are made from Hastelloy C₂₇₆ alloy to be acid resistant and they are prevented from the corrosion due to the contact with acidic fluids.

In this work, flooding scenarios are categorized in three consequent steps: synthetic brine injection, optimum acid injection, and synthetic brine injection. Brine injection scenarios (before and after acid injection) are used to restore the saturation conditions of the porous media, and measure the change in permeability before/after acid injection. Before starting the experiments, core samples are

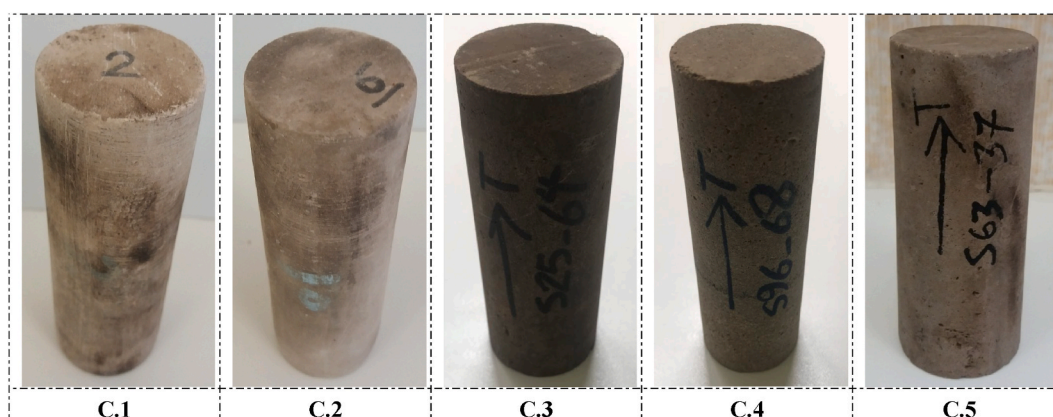


Fig. 1. Core samples used in this study.

Table 3
Composition of the core samples determined by XRD.

Core No.	Calcite (CaCO ₃)	Dolomite (CaMg(CO ₃) ₂)	Kaolinite	Quartz (SiO ₂)	Type
C.1	94 %	3 %	2 %	1 %	Calcite lime
C.2	91 %	8 %	1 %	–	Calcite lime
C.3	85 %	14 %	1 %	–	Calcite lime
C.4	93 %	2 %	3 %	2 %	Calcite lime
C.5	90 %	8 %	1 %	<1 %	Calcite lime

Table 4
Formulation of optimized acidizing package determined by different QC tests.

No.	Additive	Concentration (wt %)
1	Corrosion Inhibitor (CI)	0.40
2	Corrosion Inhibitor Intensifier (CII)	1.40
3	Anti-sludge (AS)	1.00
4	Iron Control (IC)	0.50
5	H ₂ S Scavenger (H ₂ S-S)	0.60
6	Non-emulsifier (NE)	0.45

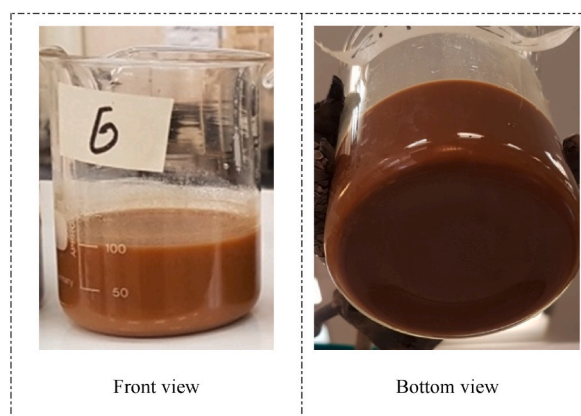


Fig. 2. Designed optimum acidizing package including all additives used for injection experiments.

Table 5
Specifications of the synthesized brine used in this study.

Parameter	Value
K ⁺ (g/L)	0.88
Na ⁺ (g/L)	37.00
Ca ²⁺ (g/L)	5.10
Mg ²⁺ (mg/L)	1
Sr ²⁺ (mg/L)	0
Fe ²⁺ (g/L)	0.013
Si ⁴⁺ (mg/L)	<20
Zn ²⁺ (mg/L)	<1
Mn ²⁺ (mg/L)	4
Ba ²⁺ (mg/L)	<10
SO ₄ ²⁻ (g/L)	0.69
Cl ⁻ (g/L)	67
HCO ₃ ⁻ (g/L)	<0.1
TDS (g/L)	112.0
pH @ amb. Temp.	7.4
SP. Gr. @ 20 °C	1.081
Salinity (g/L)	114
Conductivity (ms/cm)	175

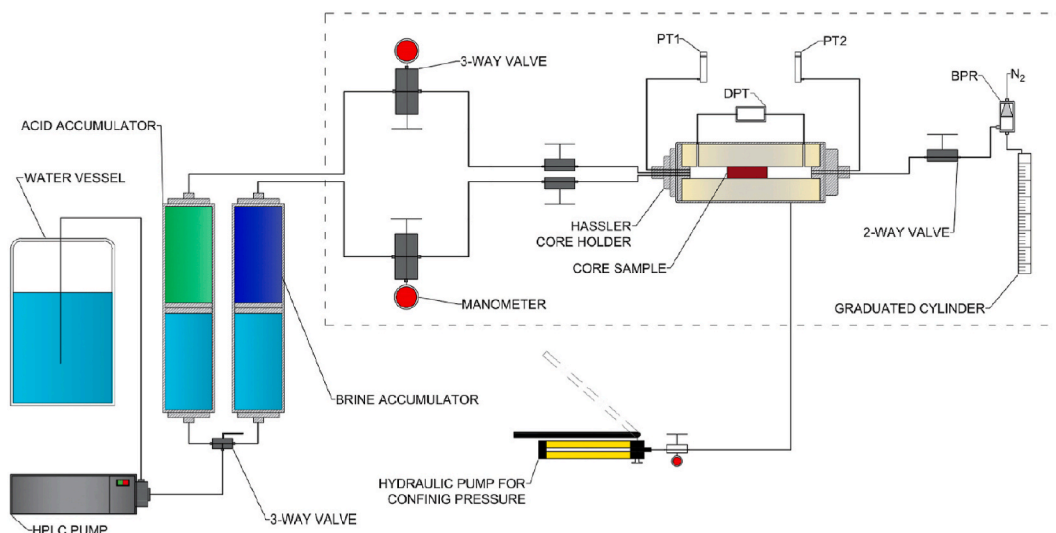


Fig. 3. Flow diagram of the core flooding experiments [96].



Fig. 4. Photograph of flooding assembly used in this work.

dried in a programmable oven for 16 h at 110 °C to remove any moisture inside the rock matrix. In all flooding experiments, confining pressure of 6.205×10^3 – 6.895×10^3 kPa was supplied using a hand pump and the pressure is fixed on the core to prevent fluid bypassing from the core sample during the experiment. All injection fluids are kept in accumulators and an oil pump (*Alemite 7783-C4*) is used to inject the fluids inside the cores at predefined rates. The core samples are evacuated and saturated with the synthetic brine (see Table 5) for porosity and permeability measurements. The porosity of the core samples was measured using the volumetric method. After complete saturation of the core, around 10 pore volume (PV) of the synthetic brine is injected into the core samples at a constant flow rate. The flow rate was fixed at 1.06×10^{-3} cm³/h. This fluid flow velocity corresponds to the laminar flow and considering capillary pressure and fluid flow through the underground reservoir porous media [71–73]. The pressure is monitored and recorded along the core sample by pressure transducer, and the initial/absolute permeability of the core sample is calculated by Darcy's law [74].

The main flooding experiments are carried out at reservoir pressure (4.482×10^4 kPa) and temperature (120 °C) and by optimum acidizing package, HCl (15 wt%). The acid injection is continued up to the breakthrough of the injected acid. Acid breakthrough is determined by monitoring the pH of the produced fluid, and/or gas detection at the outlet of the core due to the acid related chemical reactions. During the course of the experiments, N₂ supported back-pressure of about 8.273×10^3 – 9.652×10^3 kPa is applied at the low side of the core sample. Pressure drop across the core sample is continuously monitored by use of a pressure transducer. After acid injection, synthetic brine is injected to measure the change in permeability (K_f/K_i) due to the injected acid. Actually, the trend of permeability changes reveals the efficiency of the acid injection process. During the injection experiments, the effluent samples are collected and analyzed for change in calcium concentration and pH variation. Analysis of the effluent samples are performed by the inductively coupled plasma (ICP). It should be noted that some of the tests were repeated to evaluate the reproducibility and

justification of the experimental results. Regarding quantitative results, the overall trend remained unchanged. In the case of qualitative data, the overall behavior of the processes was almost similar in all the experiments. In general, the reproducibility of the results was satisfactory.

3. Results and discussion

3.1. Core samples visualization before acidizing by computed tomography (CT) scans

The CT imaging is one of the most current nondestructive methods for examining the whole cores at a submillimeter resolution. The digital images of the core can aid toward the automation of the core classification process [75]. Whole core CT scanning has a long history in helping the engineers and/or geologists to study the cores [76]. More precisely, high-resolution (micro-scale) information on the texture, composition and internal structure of the reservoir rocks can be obtained through the 2D and 3D image analysis [77]. The CT number assists us to recognize the vugs from the matrix. Actually, it represents the density of the material. Higher CT number represents materials with higher density while lower CT number represents the materials with lower density [78,79].

The CT scans of the core samples C.1 and C.5 before acidizing are shown in Figs. 5 and 6, respectively. The inlet and outlet parts of the core samples are shown in the first and last images, in the first row in Figs. 5 and 6. Middle1-3 from the left to right in the first row depict the intermediate sections of the core samples. Analysis of the all CT scans, for example Fig. 7 for C.1 and C.5 core samples, reveals that all studied core samples are heterogeneous carbonated with visible micro-porosity, and no vug is detected in the samples [80,81]. In carbonate reservoirs with heterogeneities, acid injection process reveals different behaviors compared to the homogeneous reservoirs. Thus, in this study, for reliable comparison of the different parameters during the acid injection, homogeneous core samples were utilized.

3.2. Pressure drop responses during acid injection

Experimental results are interpreted by the pressure drop behavior along the core samples during the acid injection tests, and comparison of pre- and post-acidizing CT scans. The pressure drop response during the acid injection test can be used to verify the propagation of the wormholes in the vuggy carbonate rock [82,83]. The size of the wormholes are much larger than the matrix pore sizes. The main pressure drop along the core is entirely owing to the flow streams ahead of the wormhole [82]. The pressure drop trend along the core sample during the acid injection experiments in homogeneous carbonate rock, is linear as the wormholes propagate at steady state conditions. This statement is compatible with literature data [43,82]. For example, Wang et al. (1993) showed that in acidizing of the homogeneous carbonates the pressure drop across the core often declines almost linearly as the wormhole propagates (Fig. 8) [43]. However, the pressure drop behavior during the acid injection in heterogeneous carbonate rocks is completely different from the homogenous rocks. The optimum acid injection rate depends strongly on the reservoir composition, temperature, and pore structure of the virgin rock; thus, there are no distinct rule for selection of high or low injection rate as the optimum acidizing condition [43,84].

The summary of the injection experiments and the pressure drop profile across the cores are given in Table 6 and Fig. 9,

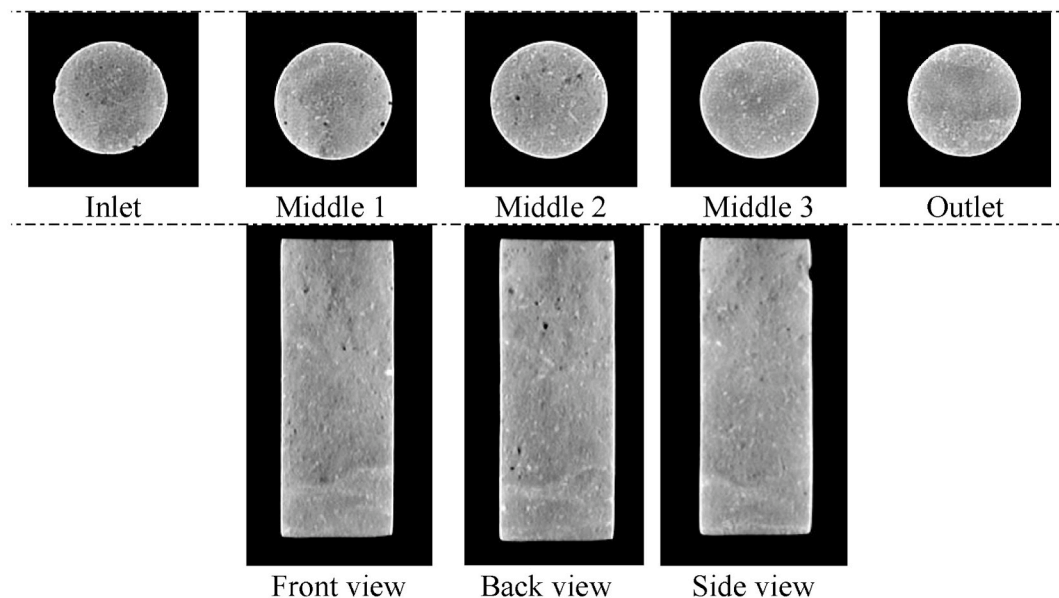


Fig. 5. Micro-CT scan photographs of core C.1; horizontal and transverse sections before acidizing.

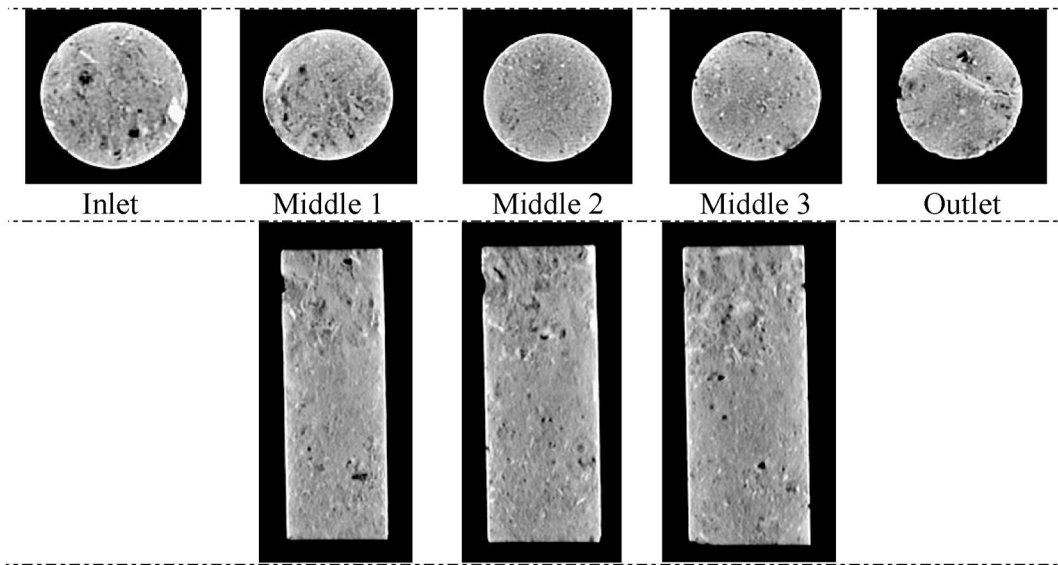
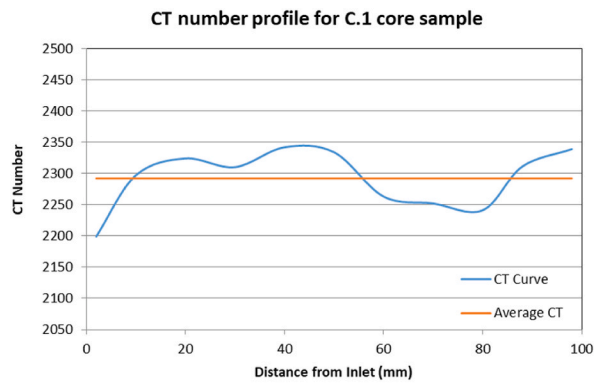
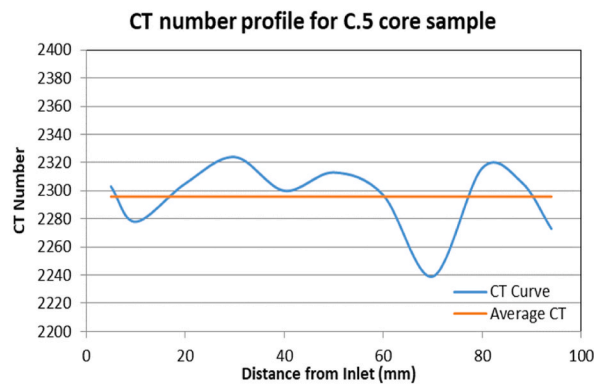


Fig. 6. CT scan images of core C.5; horizontal and transverse sections before acidizing.



(a)



(b)

Fig. 7. CT number profile of core samples before acidizing: (a) core C.1, (b) C.5; mean CT number from each image slice is used to compute a mean CT number profile.

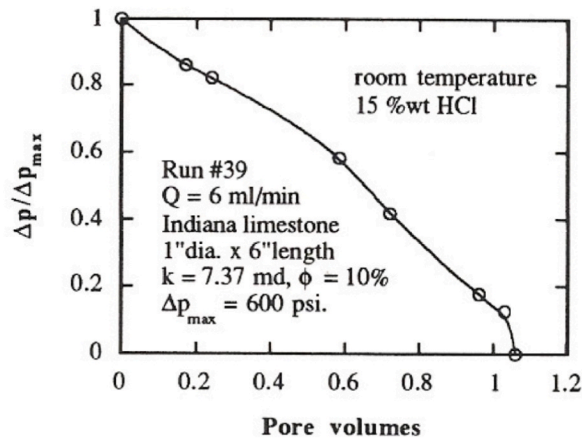


Fig. 8. Typical pressure drop profile during acid injection with Indiana limestone core, reported by Wang (1993) [43].

Table 6

Summary of the flooding experiments in different core samples.

Core No.	Injection Rate (cm ³ /min)	Air Permeability, K (md)	PV _{bt} [*] /PV	Propagated Wormhole Type
C.1	3	3.076	0.80	A single distinctive wormhole formed
C.2	1	2.320	1.4	A single wormhole with several separate branches
C.3	2	4.918	0.97	A single wormhole with several separate branches
C.4	7	5.011	0.69	A single distinctive wormhole formed
C.5	15	8.105	0.75	A single wormhole with several separate branches

respectively. The most important finding of these experiments was that the extension of the wormholes inside the core primarily depends on its permeability. Trend of the pressure drop profile is the main indicator of the wormhole creation in the rock during the acid injection. Since the size of the wormholes are very large compared to the pores of the matrix, the pressure drop in the core is totally due to the acid flow ahead of the wormholes. In acid injection experiments in relatively homogeneous carbonate rocks, when the wormholes expand at a stable speed in the core, the pressure drop across the core occurs almost linearly. As shown in Fig. 9, the pressure decreases up to the acid breakthrough for various injection rates ranging from 1 to 15 cm³/min. During the acid injection in the studied core samples, at start of the acid injection, the pressure drop increased because of the higher viscosity of acid solution, the CO₂ gas released owing to the acid reaction with the rock, and/or the precipitation of the iron; then, the pressure drop reduced gradually due to the continuous extension of the acid wormholes within the rock matrix. Finally, the pressure drop stabilized, and dropped to a near zero value. For successful acidizing jobs, final pressure drop should be sufficiently less than the initial pressure drop, almost half the initial pressure drop. It indicates that the final permeability is improved although some iron precipitation may be occurred. If the final pressure drop be approximately the same as the initial pressure drop, the acidizing job fails, and the final permeability remains nearly the same as the initial permeability. In Fig. 10, core C.2, due to the low initial permeability (i.e. low rock injectivity) and low injection rate, the inlet face of the core has been corroded due to the iron precipitation; finally, acid breakthrough has occurred after injecting 1.4 pore volume. In this situation, the wormholes have not been well extended within the core matrix, and they have been created at the wall of the core (Fig. 10b). Obtained results in this section are in line with the previous studies [85–87]. In Fig. 10, the photos of inlet, outlet, and side views of the core samples after acidizing process are depicted.

3.3. Effect of initial permeability and injection rate on efficiency of acidizing process

The permeabilities of the core samples before and after acidizing tests are measured and given in Table 7. The permeability of the all core samples except core C.2 has been greatly improved after acidizing, which reveals effective stimulation process in the studied carbonate cores. For core sample C.2, the permeability after acidizing (K_f) has increased 1.5 times the initial permeability before acidizing (K_i), which is the lowest permeability improvement among the tested cores. As discussed before, poor acidizing in this sample is attributed to the much lower injectivity of the core in comparison to the other core samples. As the results of permeability measurements before and after acidizing show (Table 7), there is no significant relation between the initial permeability of the cores and efficiency of the stimulation process [88,89].

The main factors which influence the extension of the wormholes within a rock type are acid type, rock structure and composition, acid injection rate, temperature, pressure, etc [90]. However, the acid injection rate is key factor for a specific type of acid and rock [42,91]. It has been commonly approved that the surface dissolution type is formed under a low acid injection rate, uniform dissolution type under a high acid injection rate, and a wormhole is developed at a medium injection rate [92,93]. As given in Tables 6 and in this work, acid injection rates are in the range of 1–15 cm³/min. The acid breakthrough volume vs. acid injection rate is displayed in

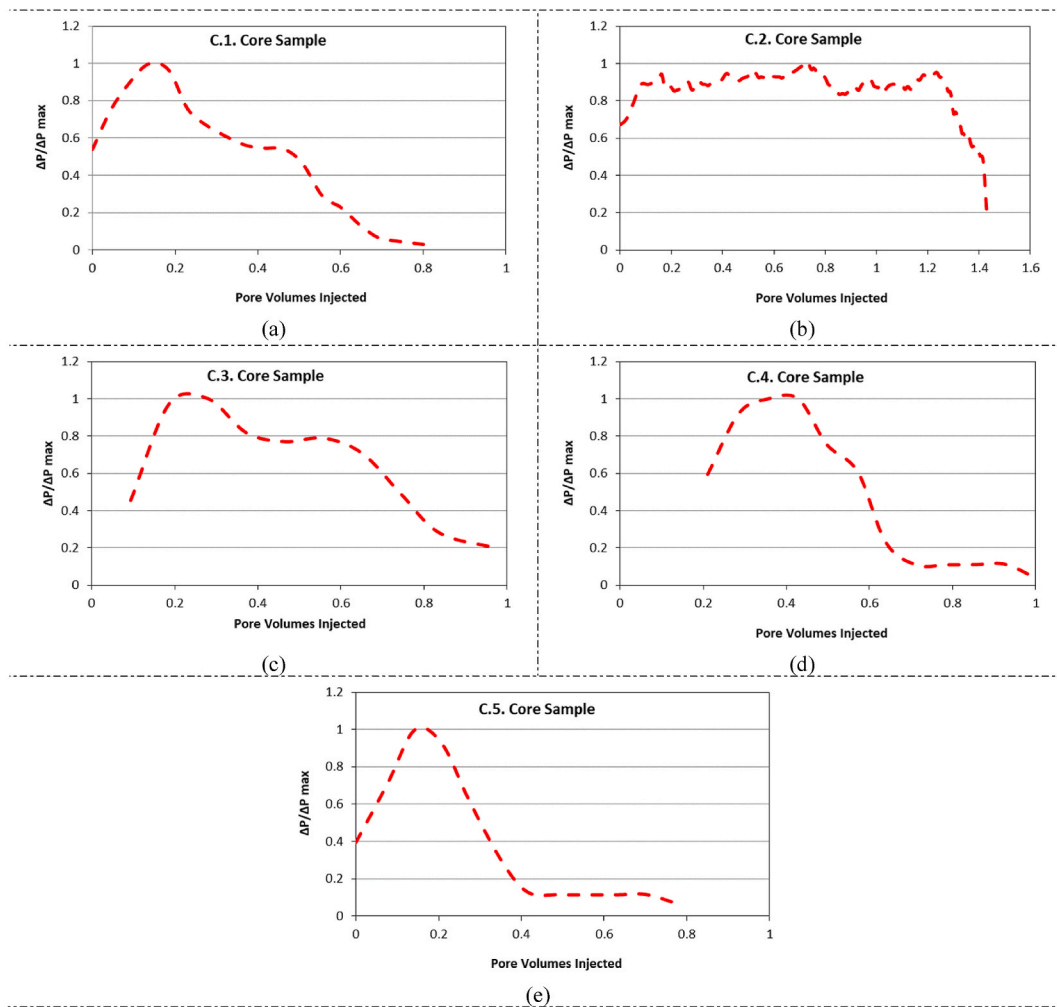


Fig. 9. Pressure drop response versus injected acid pore volume (PV) along the core samples during acid injection: (a) C.1, (b) C.2, (c) C.3., (d) C.4., (e) C.5.

Fig. 11. It is obvious from Fig. 11 that the smallest volume of acid at breakthrough time has occurred at injection rate of $7 \text{ cm}^3/\text{min}$, in core C.4. In this case, the minimum acid volume has been spent for stimulation process. The variations in permeability values during the acid stimulation process at different injection rates are shown in Fig. 12. As well, these data, permeability changes versus injection rates, are given in Table 7. Based on the obtained data, the maximum permeability enhancement is attained at injection rate of $7 \text{ cm}^3/\text{min}$, which corresponds to the minimum volume of the acid at breakthrough time, as discussed before in Fig. 11. Thus, for the range of experiments performed here, injection rate of $7 \text{ cm}^3/\text{min}$ in the core sample C.4 is considered as the optimal acid injection rate. The optimum acid injection rate obtained here is in the range of the others' works [42,43,53].

3.4. CT scan analysis of core samples after acidizing process

The core samples were acidized, resulting in the formation of wormholes, as shown in the CT-scan analysis and 3D simulated images in Fig. 13. The Avizo package was utilized to simulate the 3D model of the core samples and created wormholes. Fig. 13 indicates that the path created in the core sample C.4 has a shorter length and fewer branches than the other samples, which is close to the optimal state. Within the core, there exists a single distinctive and uniform wormhole due to the nearly fixed diameter of the wormholes that have been developed. Due to the low injection rate in sample C.3, a conic-like pathway has been developed which is confirmed by simulated image. It is worth mentioning that the created wormhole in sample C.2 is a mixture of the face dissolution and conical with numerous branches. Formation of these patterns is ascribed to the partial corrosion of the entrance surface and part of the core sample wall. Actually, in the beginning of the acid injection, the inlet face of the core is severely dissolved in HCl acid. In sample C.5, as the injection rate is much higher than the optimum rate, a ramified/branching wormhole pattern has been created, and the extension of the wormhole was continued fast to the outlet face of the core. This fast process reveals the rapid consumption of HCl-acid fluid as a result of the high acid injection rate. It should be noted that high injection rate resulted in many densely distributed small



Fig. 10. Inlet, outlet, and side views of tested cores after acidizing: (a) C.1, (b) C.2, (3) C.3, (d) C.4, (e) C.5.

Table 7
Injection rates and permeability changes before/after the acidizing process.

Core No.	Injection Rate (cm ³ /min)	Initial Permeability with 2 % KCl, K _i (md)	Final Permeability with 2 % KCl, K _f (md)	K _f /K _i
C.1	3	2.30	7.82	3.4
C.2	1	1.88	2.82	1.5
C.3	2	4.50	34.20	7.6
C.4	7	4.63	51.86	11.2
C.5	15	6.46	45.87	7.1

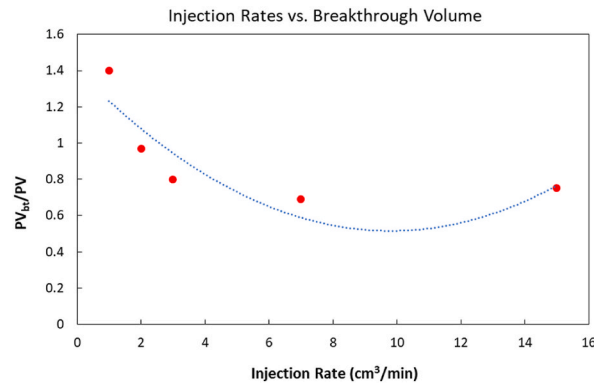


Fig. 11. Acid efficiency curve: injection rate versus acid breakthrough volume.

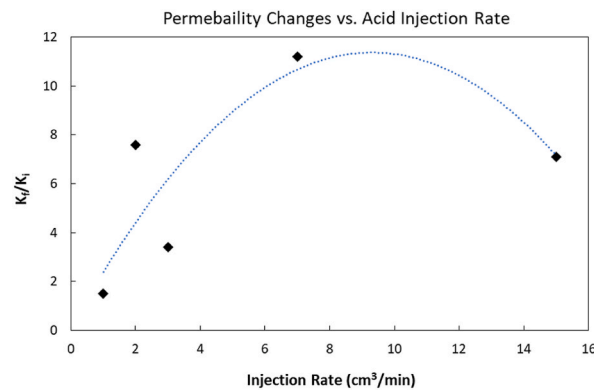


Fig. 12. Permeability changes during acid stimulation process at different injection rates.

holes around the main hole in the inlet face of the core. However, the CT-scan analysis of the outlet surface and simulated image in Fig. 13 demonstrate the formation of only a single wormhole, and the small holes are distributed only on the entrance surface of core sample C.5. Therefore, the small hole formed at the entrance cannot form a complete wormhole until it reaches the exit surface of the core sample.

3.5. Calcium ion and pH analysis of core effluent samples

Fig. 14 depicts the calcium ion concentration (Ca²⁺), measured by ICP technique, in effluent fluid corresponding to the injection experiments in the core samples. The content of calcium ion depends on the amount of dissolved rock by HCl which is greater for longer contact time with the acid. The minimum calcium concentration (19,547 ppm) was achieved at optimum injection rate (7 cm³/min). The optimum injection rate is corresponded to the minimum acid-rock contact time which results in stable extension of the wormhole within the core sample. The maximum calcium concentration during the acid injection experiments was observed for the smallest and greatest injection rates (1 and 15 cm³/min). The calcium concentration for the injection rates of 1 and 15 cm³/min are 24,034 and 23167 ppm, respectively. It can be concluded that the maximum contact time and maximum contact area between the acid and rock are achieved at minimum and maximum acid injection rates, respectively.

The pH values of the effluent samples during the acid injection experiments versus injected acid pore volume and at different injection rate are shown in Fig. 15. The results show that the pH value of the effluent fluid sample is related to the acid injection rate. By

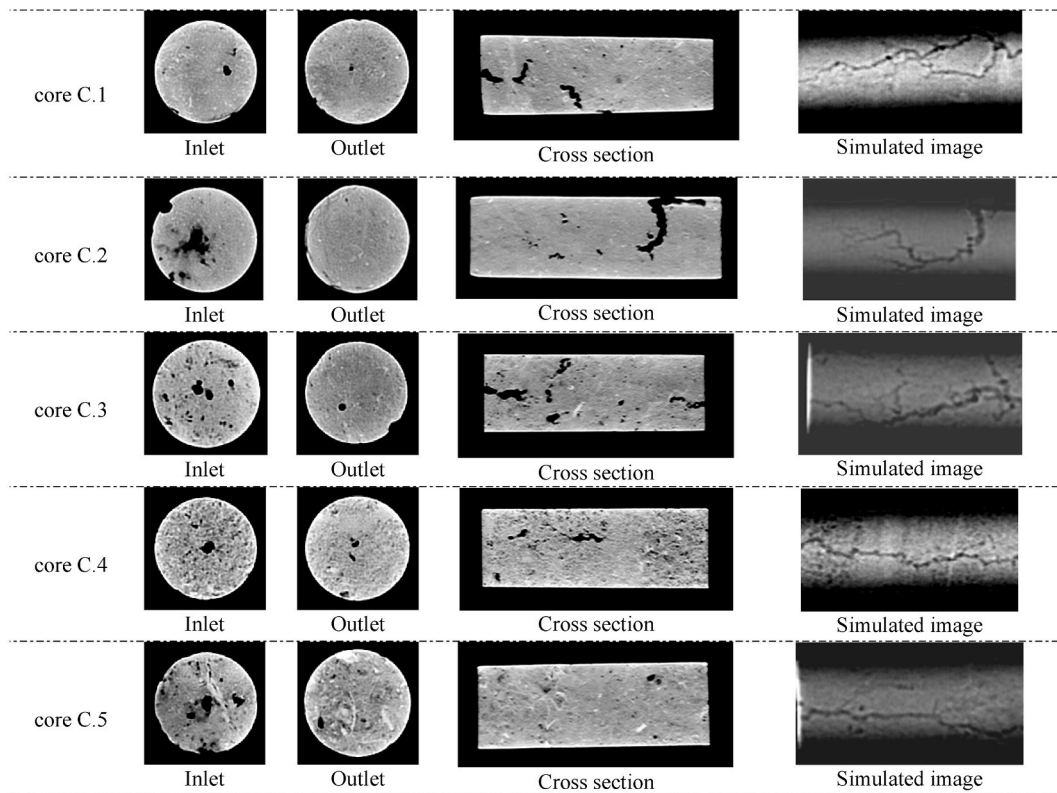


Fig. 13. Column 1–3: Micro-CT scan photographs of core samples after acidizing process; column 4: 3-D simulated images of created wormholes in the core samples after acidizing process, 3-D visualization of the core samples was performed by Avizo package.

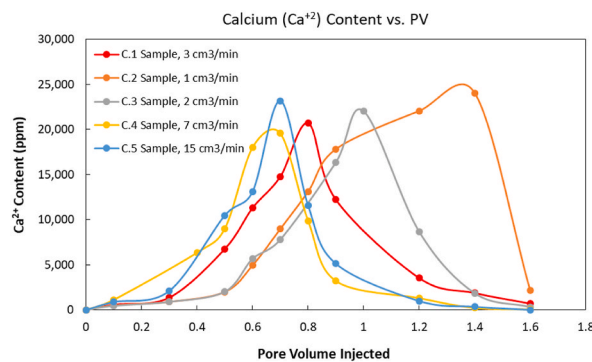


Fig. 14. Calcium (Ca²⁺) concentration in the core effluent sample at different injection rates.

increasing the acid injection rate, the time for acid to spend upon contacting with rock decreases; therefore, the value of pH decreases. The lowest pH value (0.28) is attained for the highest injection rate, 15 cm³/min. For all injection rates, the pH value decreases down to a minimum value corresponding to the volume of acid breakthrough. After breakthrough of acid, the pH value increases by starting the water injection [94,95]. Results obtained for volume of breakthrough are consistent with the previously described breakthrough analysis obtained by the pressure decline profile.

4. Conclusions

Here, responsible mechanisms for the development and extension of the ramified wormholes within the carbonate core samples were comprehensively investigated through HP-HT injection experiments and CT scan imaging of the cores before/after acidizing process. In addition, the effects of various acid injection rates (1–15 cm³/min) on the wormholes propagation and changes of the rock permeability were examined. It was found that the extension of the wormholes inside the core mainly depends on its permeability.

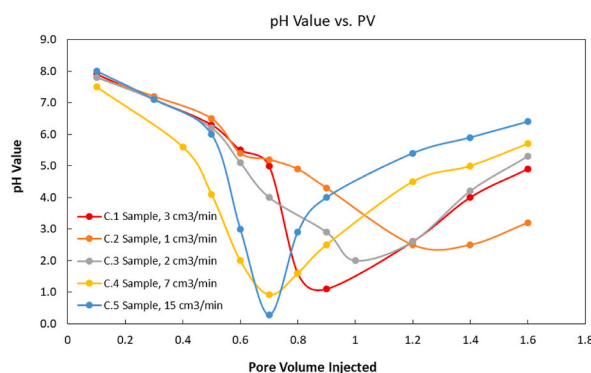


Fig. 15. pH values in the core effluent sample at different injection rates.

During the acidizing treatment of the carbonate rocks, pressure drop profile can be used for prediction of the point of wormhole creation in the rock. A sudden decrease in the pressure drop versus injected acid pore volume over a short period of time is attributed to the formation of wormholes in the core. Based on the obtained HP-HT results, the initial permeability of the cores doesn't affect the performance of the acid stimulation process. For the range of experiments conducted here, the optimum acid injection rate was found to be $7 \text{ cm}^3/\text{min}$ corresponding to the minimum volume of the acid at the breakthrough time. The highest permeability enhancement ($K_f/K_i = 11.2$) for performed acid treatments was attained at optimum acid injection rate in the core sample C.4. The concentration of the calcium in the effluent fluids was 24,034 and 23167 ppm for the injection rates of 1 and $15 \text{ cm}^3/\text{min}$, respectively. Consequently, the minimum and maximum acid injection rates are corresponded to the maximum contact time and highest contact area between the acid and rock, respectively. The acidizing operation in carbonated reservoirs will be only effective if the final pressure drop along the core sample is less than the initial pressure drop. Otherwise, the acidizing job fails at high cost and damaging side-effects. As the experiments have been performed at operation conditions of pressure and temperature, the findings of this study can be used as a worthy guide to successfully design and implement stimulation jobs in similar reservoirs. However, due to the some limitations in providing more reservoir rock samples and various acidizing packages, further research studies are essential for better supporting of the analyses and acquired experimental data in this work. The obtained results may serve as an effective and reliable roadmap for future studies.

Data availability statement

Has data associated with your study been deposited into a publicly available repository? No. Data will be made available on request.

CRediT authorship contribution statement

Saber Mohammadi: Writing – review & editing, Writing – original draft, Visualization, Supervision, Methodology, Investigation, Formal analysis, Conceptualization.

Declaration of competing interest

The authors declare that they have no known competing financial interests or personal relationships that could have appeared to influence the work reported in this paper.

Nomenclatures

Ca^{+2}	Calcium ion
CaCO_3	Calcium carbonate
$\text{CaMg}(\text{CO}_3)_2$	Dolomite
CH_3COOH	Acetic acid
cm^3/min	Flow rate in cubic centimeter per minute
CO_2	Carbon dioxide
CT	Computed tomography
HCl	Hydrochloric acid
HF	Hydrofluoric acid
HP-HT	High pressure-high temperature
ICP	Inductively coupled plasma

K_i	Initial permeability (before acidizing)
K_f	Final permeability (after acidizing)
mD	millidarcy
ppm:	part per million
psi	Pounds per square inch
PV	Pore volume
PVBT	Pore volume to breakthrough
°F	Temperature reported in Fahrenheit
QC	Quality control
SiO ₂	Quartz
XRD	X-ray powder diffraction
Wt%	Percentage by weight
μm	Microns

References

- [1] P. Rae, G.D. Lullo, Matrix acid stimulation-A review of the state-of-the-Art, The Hague, The Netherlands, in: SPE European Formation Damage Conference, 2003 (SPE-82260-MS).
- [2] H.H. Abass, A.A. Al-Mulhem, M.S. Alqam, K.R. Mirajuddin, Acid fracturing carbonate-rich shale: a Feasibility investigation of Eagle ford formation, San Antonio, Texas, USA, in: SPE Annual Technical Conference and Exhibition, September 2006. SPE-102590-MS.
- [3] R. Cash, D. Zhu, A.D. Hill, Acid fracturing carbonate-rich shale: a feasibility investigation of eagle ford formation, Beijing, China, in: SPE Asia Pacific Hydraulic Fracturing Conference, August 2016 (SPE-181805-MS).
- [4] J. Deng, A.D.D. Hill, D. Zhu, A theoretical study of acid-fracture conductivity under closure stress, SPE Prod. Oper. 26 (1) (2011) 9–17 (SPE-124755-PA).
- [5] M.A. Al-Rekabi, A. Aktebanee, A.S. Al-Ghaffari, T. Saleem, Carbonate matrix acidizing efficiency from acidizing induced skin point of view: case study in majnoon oilfield, in: International Petroleum Technology Conference, 2020 (IPTC-20006-MS).
- [6] A.I. Rabie, M.R. Saber, H.A. Nasr El-Din, A new environmentally friendly acidizing fluid for HP/HT matrix acidizing treatments with enhanced product solubility, The Woodlands, Texas, USA, in: SPE International Symposium on Oilfield Chemistry, April 2015 (SPE-173751-MS).
- [7] A. Almalichy, Z. Turzó, U. Alameedy, Carbonate Rock Matrix Acidizing: A Review of Acid Systems and Reaction Mechanisms, Tavaszi Szél Konferencia At, Budapest, Hungary, 2022.
- [8] B.B. Williams, J.L. Gidley, R.S. Schechter, Acidizing Fundamentals, Henry L. Doherty Memorial Fund of AIME, Society of Petroleum Engineers of AIME, 1979.
- [9] Y. Li, F. Zhou, B. Li, T. Cheng, M. Zhang, Q. Wang, E. Yao, T. Liang, Optimization of fracturing fluid and retarded acid for stimulating tight naturally fractured bedrock reservoirs, ACS Omega 7 (29) (2022) 25122–25131.
- [10] M.S. Aljawad, Mineralogy impact on acid fracture design in naturally fractured carbonates, ACS Omega 8 (13) (2023) 12194–12205.
- [11] Z. Zhao, Y. Ma, Y. Zhang, K. Lan, X. Zhang, Evaluation and application of efficient gelled acid for carbonate formation fracturing, ACS Omega 8 (29) (2023) 26201–26205.
- [12] A. Hashemi, Acid Fracturing Treatment in an Iranian Carbonated Reservoir, 21st World Petroleum Congress, Moscow, Russia, June 2014 (WPC-21-2094).
- [13] J. Guo, B. Gou, N. Qin, J. Zhao, L. Wu, K. Wang, J. Ren, An innovative concept on deep carbonate reservoir stimulation: three-dimensional acid fracturing technology, Nat. Gas. Ind. B 7 (5) (2020) 484–497.
- [14] R. Zhang, B. Hou, B. Zhou, Y. Liu, Y. Xiao, K. Zhang, b effect of acid fracturing on carbonate formation in southwest China based on experimental investigations, J. Nat. Gas Sci. Eng. 73 (2020) 103057.
- [15] K. Pourabdollah, Matrix acidizing: a fouling mitigation process in oil and gas wells, Rev. Chem. Eng. 36 (2) (2020) 311–331.
- [16] A.A. Garrouch, A.R. Jennings, A contemporary approach to carbonate matrix acidizing, J. Pet. Sci. Eng. 158 (2017) 129–143.
- [17] A. Al-Arji, A. Al-Azman, F. Le-Hussain, K. Regenauer-Lieb, Acid stimulation in carbonates: a laboratory test of a wormhole model based on damköhler and péclet numbers, J. Pet. Sci. Eng. 203 (2021) 108593.
- [18] K. Dong, A new wormhole propagation model at optimal conditions for carbonate acidizing, J. Pet. Sci. Eng. 171 (2018) 1309–1317.
- [19] U. Alameedy, A. Fatah, A.K. Abbas, A. Al-Yaseri, Matrix acidizing in carbonate rocks and the impact on geomechanical properties: a review, Fuel 349 (2023) 128586.
- [20] B. Bazin, From matrix acidizing to acid fracturing: a laboratory evaluation of acid/rock interactions, SPE Prod. Facil. 16 (1) (2001) 22–29.
- [21] M.P. Schwalbert, M.S. Aljawad, A.D. Hill, D. Zhu, Decision criterion for acid-stimulation method in carbonate reservoirs: matrix acidizing or acid fracturing? SPE J. 25 (5) (2020) 2296–2318.
- [22] M.J. Economides, K.G. Nolte, Reservoir Stimulation, third ed., Prentice Hall, Englewood Cliffs, 2001.
- [23] T.W. Teklu, H.H. Abass, R. Hanashmoon, J.C. Carratu, M. Ermila, Experimental investigation of acid imbibition on matrix and fractured carbonate rich shales, J. Nat. Gas Sci. Eng. 45 (2017) 706–725.
- [24] R.S. Aboud, K.L. Smith, L. Forero Pachon, L.J. Kalfayan, Effective matrix acidizing in high-temperature environments, Anaheim, California, U.S.A., in: SPE Annual Technical Conference and Exhibition, November 2007. SPE 109818-MS
- [25] M.U. Shafiq, H.K.B. Mahmud, Sandstone matrix acidizing knowledge and future development, J. Pet. Explor. Prod. Technol. 7 (2017) 1205–1216.
- [26] S. Al-Harthy, Options for high-temperature well stimulation, Oilfield Rev 20 (2009) 52–62. Schlumberger.
- [27] S.S. Abdelmoneim, H.A. Nasr-El-Din, Determining the optimum HF concentration for stimulation of high temperature sandstone formations, Budapest, Hungary, in: SPE European Formation Damage Conference and Exhibition, June 2015 (SPE-174203-MS).
- [28] G. Zimmermann, G. Blöcher, A. Reinicke, W. Brandt, Rock specific hydraulic fracturing and matrix acidizing to enhance a geothermal system - concepts and field results, Tectonophysics 503 (1–2) (2011) 146–154.
- [29] B.G. Al-Harbi, M.N. Al-Dahlan, M.H. Al-Khaldi, A.M. Al-Harith, A.K. Abadi, Evaluation of organic hydrofluoric acid mixtures for sandstone acidising, Beijing, China, in: International Petroleum Technology Conference, March 2013 (SPE IPTC-16967-MS).
- [30] N. Li, F.B. Zeng, J. Li, Q. Zhang, Y. Feng, P. Liu, Kinetic mechanics of the reactions between HCl/HF acid mixtures and sandstone minerals, J. Nat. Sci. Gas. Eng. 34 (2016) 792–802.
- [31] S. Portier, F.D. Vuataz, Developing the ability to model acid-rock interactions and mineral dissolution during the RMA stimulation test performed at the soultz-sous-forêts EGS site, France, C. R. Geosci. 342 (7–8) (2010) 668–675.
- [32] M. Dargi, E. Khamehchi, J. Mahdavi Kalatehno, Optimizing acidizing design and effectiveness assessment with machine learning for predicting post-acidizing permeability, Sci. Rep. 13 (2023) 11851.
- [33] Sarai, et al., Acidizing treatment design assessment based on dolomitic field core testing, Lafayette, Louisiana, USA, in: SPE International Conference and Exhibition on Formation Damage Control, February 2022 (SPE-208824-MS).

- [34] R.L. Thomas, A. Saxon, A.W. Milne, The use of coiled tubing during matrix acidizing of carbonate reservoirs completed in horizontal, deviated, and vertical wells, *SPE Prod. Facil.* 13 (1998) 147–162 (SPE-50964-PA).
- [35] G. Nitters, L. Roodhart, H. Jongma, V. Yeager, M. Buijse, D. Fulton, J. Dahl, E. Jantz, Structured approach to advanced candidate selection and treatment design of stimulation treatments, Dallas, Texas, in: *SPE Annual Technical Conference and Exhibition*, October 2000 (SPE-63179-MS).
- [36] H. Jafarpour, D.G. Petrakov, A. Khorrali, A.S. Galtcova, Design and optimization of matrix acidizing in a Middle East carbonate reservoir, in: *7th EAGE Saint Petersburg International Conference and Exhibition*, Apr 2016 cp-480-00071.
- [37] L. Kalfayan, *Production Enhancement with Acid Stimulation*, 9781593701390, Penn Well Publish, 2008. ISBN, 159370139X, 9781593701390.
- [38] A.D. Hill, R.S. Schechter, Fundamentals of acid stimulation, in: M.J. Economides, K.G. Nolte (Eds.), *Reservoir Stimulation*, third ed., Wiley Chichester, 2000, pp. 1–28.
- [39] A. Ortega, H.A. Nasr-El-Din, Acidizing high temperature carbonate reservoirs using methanesulfonic acid: a coreflood study, Houston, Texas, in: *AADE Fluids Technical Conference and Exhibition*, 2014.
- [40] A. Katende, F. Sagala, A critical review of low salinity water flooding: mechanism, laboratory and field application, *J. Mol. Liq.* 278 (2019) 627–649.
- [41] P. Mwangi, P.V. Brady, M. Radonjic, G. Thyne, The effect of organic acids on wettability of sandstone and carbonate rocks, *J. Pet. Sci. Eng.* 165 (2018) 428–435.
- [42] N. Qi, B. Li, G. Chen, M. Fang, X. Li, C. Liang, Optimum fluid injection rate in carbonate acidizing based on acid dissolution morphology analysis, *Energy & Fuels* 31 (12) (2017) 13448–13453.
- [43] Y. Wang, A.D. Hill, R.S. Schechter, The optimum injection rate for matrix acidizing of carbonate formations, Houston, Texas, in: *SPE Annual Technical Conference and Exhibition*, October 1993. SPE-26578-MS.
- [44] E. Rabbani, A. Davarpanah, M. Memariani, An experimental study of acidizing operation performances on the wellbore productivity index enhancement, *J. Pet. Explor. Prod. Technol.* 8 (2018) 1243–1253.
- [45] C.N. Fredd, H.S. Fogler, Optimum conditions for wormhole formation in carbonate porous media: influence of transport and reaction, *SPE J.* 4 (3) (1999) 196–205 (SPE-56995-PA).
- [46] R. Safari, F. Fragachan, C.S. Smith, Analysis of critical operational and reservoir parameters in carbonate acidizing design, Garden Grove, California, USA, in: *SPE Western Regional Meeting*, April 2018 (SPE-190094-MS).
- [47] Q. Sahu, M. Fahs, H. Hoteit, Optimization and uncertainty quantification method for reservoir stimulation through carbonate acidizing, *ACS Omega* 8 (1) (2023) 539–554.
- [48] H.A. Nasr-El-Din, M.M. Samuel, S.K. Kelkar, Investigation of a new single-stage sandstone acidizing fluid for high temperature formations, Scheveningen, The Netherlands, in: *European Formation Damage Conference*, 2007 (SPE-107636-MS).
- [49] J. Guo, L. Zhan, B. Gou, J. Zeng, C. Zhou, Experimental optimization of acid system for acidizing in mud-damaged deep fractured carbonate formation, *J. Pet. Sci. Eng.* 195 (2020) 107639.
- [50] V.H. Leong, H.B. Mahmud, M.C. Law, H.C.Y. Foo, I.S. Tan, A comparison and assessment of the modelling and simulation of the sandstone matrix acidizing process: a critical methodology study, *J. Nat. Gas Sci. Eng.* 57 (2018) 52–67.
- [51] A.H.H. Al-Ghamdi, M.A. Mahmoud, G. Wang, A.D.D. Hill, H.A.A. Nasr-El-Din, Acid diversion by use of viscoelastic surfactants: the effects of flow rate and initial permeability contrast, *SPE J.* 19 (2014) 1203–1216.
- [52] X. Hu, S. Hu, F.F. Jin, S. Huang, *Physics of Petroleum Reservoirs*, Springer, 2017, 978-3-662-53282-9.
- [53] Z. Sidaoui, A. Abdulazeez, M. Abbas, Prediction of optimum injection rate for carbonate acidizing using machine learning, in: *SPE Kingdom of Saudi Arabia Annual Technical Symposium and Exhibition*, Dammam, Saudi Arabia, April 2018 (SPE-192344-MS).
- [54] M.A. Sayed, A.J. Cairns, F.F. Chang, Boosting reaction rate of acids for better acid fracturing stimulation of dolomite-rich formations, *SPE J.* 28 (2023) 1690–1705 (SPE-214319-PA).
- [55] R. Ahmadi, B. Aminshahidi, J. Shahrazi, Data-driven analysis of stimulation treatments using association rule mining, *SPE Prod. Oper.* 38 (2023) 552–564 (SPE-214699-PA).
- [56] C. Jia, S. Alkaabi, K. Sepehrnoori, D. Fan, J. Yao, Numerical modeling and studies of the acid stimulation process in dolomite carbonate rocks, *SPE J.* (2023) 1–21 (SPE-215820-PA).
- [57] Q. Sahu, M. Fahs, H. Hoteit, Investigating acidizing in carbonate reservoirs: global sensitivity analysis, Galveston, Texas, USA, in: *SPE Reservoir Simulation Conference*, 2023 (SPE-212222-MS).
- [58] A. Al-Otaibi, An investigation into the roles of chlorides and sulphate salts on the performance of low-salinity injection in sandstone reservoirs: experimental approach, *J. Pet. Explor. Prod. Technol.* 10 (2020) 2857–2871.
- [59] C. McPhee, J. Reed, I. Zubizarreta, Chapter 4 - core sample preparation, *Dev. Petrol. Sci.* 64 (2015) 135–179.
- [60] R. Farokhpoor, L. Sundal, A. Skjærstein, A. Hebing, X. Zhang, L. Pirlea, Core cleaning and wettability restoration – selecting appropriate method, in: *The 35th International Symposium of the Society of Core Analysts*, September 2021.
- [61] **Britannica**, The editors of encyclopaedia. “Core sampling”, *Encyclopedia Britannica*. (Accessed 5 Feb 2018).
- [62] H.S. Birkett, *Core Sampling Recommended Procedures*, Audubon Sugar Institute Louisiana State University Agricultural Center, 1998.
- [63] C. Zhou, L. Li, R. Zeng, W. Chen, Y. Liu, Spontaneous imbibition in igneous rocks: effect of KCl concentration, confining pressure, and imbibition direction, *J. Pet. Explor. Prod. Technol.* 10 (2020) 3227–3234.
- [64] S.S. Al-Jaroudi, A. Ul-Hamid, A.I. Mohammed, S. Saner, Use of X-ray powder diffraction for quantitative analysis of carbonate rock reservoir samples, *Powder Technol.* 175 (3) (2007) 115–121.
- [65] R. Khalil, H. Emadi, F. Altawati, Investigating the effect of matrix acidizing injection pressure on carbonate-rich marcellus shale core samples: an experimental study, *J. Pet. Explor. Prod. Technol.* 11 (2021) 725–734.
- [66] A. Ahmadi, K. Paydar, A. Ebadi, M. Manteghian, Study and optimization of the effect of temperature, acid concentration, and rock grain size on the pH of carbonate reservoir acidizing, *J. Chem. Pet. Eng.* 56 (2) (2022) 331–339.
- [67] L. Scoppio, P. Nice, G. Mortali, Intiso, P. Luciana, I. Eugenio, H. Nasvik, J. Cassidy, A. Hisashi, Testing of stimulation acidizing packages on high strength corrosion resistant tubing alloys for high pressure deep water wells, San Antonio, Texas, USA, in: *CORROSION Conference 2014*, 2014. NACE-2014-3945).
- [68] S.J.M. Jeffry, K. Trjanganung, A.A. Chandrakant, B. Madon, A. Katende, I. Ismail, Selection of suitable acid chemicals for matrix stimulation: a Malaysian Brown field scenario, *J. Pet. Sci. Eng.* 186 (2020) 106689.
- [69] A. Zeinolabedini Hezave, S. Dorostkar, S. Ayatollahi, M. Nabipour, B. Hemmateenejad, Mechanistic investigation on dynamic interfacial tension between crude oil and ionic liquid using mass transfer concept, *J. Dispersion Sci. Technol.* 35 (10) (2014) 1483–1491.
- [70] Y. Chen, N.K. Jha, D. Al-Bayati, M. Lebedev, M. Sarmadivaleh, S. Iglauer, A. Saeedi, Q. Xie, Geochemical controls on wettability alteration at pore-scale during low salinity water flooding in sandstone using X-ray micro computed tomography, *Fuel* 271 (2020) 117675.
- [71] F. Siddiqui, M.Y. Soliman, W. House, et al., Pre-Darcy flow revisited under experimental investigation, *J. Anal. Sci. Technol.* 7 (2) (2016).
- [72] G. Medici, L.J. West, S.A. Banwart, Groundwater flow velocities in a fractured carbonate aquifer-type: implications for contaminant transport, *J. Contam. Hydrol.* 222 (2019) 1–16.
- [73] G. Longmuir, Pre-Darcy Flow: A Missing Piece of the Improved Oil Recovery Puzzle? *SPE/DOE Symposium on Improved Oil Recovery*, Tulsa, Oklahoma, April 2004 (SPE-89433-MS).
- [74] J.C. Manning, *Applied Principles of Hydrology*, third ed., Prentice Hall, 1997, p. 276.
- [75] K. Chawshin, C.F. Berg, D. Varagnolo, O. Lopez, Lithology classification of whole core CT scans using convolutional neural networks, *SN Appl. Sci.* 3 (2021) 668.
- [76] K. Chawshin, A. Gonzales, C.F. Berg, D. Varagnolo, Z. Heidari, O. Lopez, Classifying lithofacies from textural features in whole-core CT-scan images, *SPE Reservoir Eval. Eng.* 24 (2) (2021) 341–357.

- [77] U. Odi, T. Nguyen, Geological facies prediction using computed tomography in a machine learning and deep learning environment, in: Unconventional Resources Technology Conference, Society of Exploration Geophysicists, 2018, pp. 336–346. URTEC-2901881-MS.
- [78] A. Abdulraheem, Impact of HCl acidizing treatment on mechanical integrity of carbonaceous shale, *ACS Omega* 7 (16) (2022) 13629–13643.
- [79] A.F. Ibrahim, A novel retarded HCl acid system for HPHT carbonate acidizing applications: experimental study, *can. J. Chem. Eng.* 100 (6) (2022) 1158.
- [80] S. Allshorn, R.A. Dawe, C.A. Grattoni, Implication of heterogeneities on core porosity measurements, *J. Pet. Sci. Eng.* 174 (2019) 486–494.
- [81] W. Li, X. Liu, L. Liang, Y. Zhang, X. Li, J. Xiong, Pore-structural characteristics of tight fractured-vuggy carbonates and its effects on the P- and S-wave velocity: a micro-CT study on full-diameter cores, *Energies* 13 (2020) 6148.
- [82] O. Izgec, Reactive Flow in Vuggy Carbonate: Method and Models Applied to Matrix Acidizing of Carbonates, PhD Thesis, Texas A&M University, May 2009.
- [83] H. Yoo, Y. Kim, H. Jang, J. Lee, Propagation characteristics of optimum wormhole in carbonate matrix acidizing using micro X-ray CT imaging, *J. Pet. Sci. Eng.* 196 (2021) 108010.
- [84] A. Mustafa, T. Alzaki, M. Saleh Aljawad, T. Solling, J. Dvorkin, Impact of acid wormhole on the mechanical properties of chalk, limestone, and dolomite: experimental and modeling studies, *Energy Rep.* 8 (2022) 605–616.
- [85] A.J. Cairns, K.L. Hull, M. Sayed, From design to practice: development of new acid platforms to address upstream oil and gas production challenges, *Chemistry Solutions to Challenges in the Petroleum Industry* 3–21 (2019).
- [86] A.B.G. Motta, R.L. Thompson, J.L. Favero, R.A.C. Dias, L.F.L.R. Silva, F.G. Costa, M.P. Schwalbert, Rheological effects on the acidizing process in carbonate reservoirs, *J. Pet. Sci. Eng.* 207 (2021) 109122.
- [87] P. Liu, X. Yan, J. Yao, S. Sun, Modeling and analysis of the acidizing process in carbonate rocks using A two-phase thermal-hydrologic-chemical coupled model, *Chem. Eng. Sci.* 207 (2019) 215–234.
- [88] H. Jafarpour, J. Moghadasi, A. Khormali, D.G. Petrakov, R. Ashena, Increasing the stimulation efficiency of heterogeneous carbonate reservoirs by developing a multi-batched acid system, *J. Pet. Sci. Eng.* 172 (2019) 50–59.
- [89] F. Yang, Sensitivity evaluation and stimulation optimization of ultralow permeability sandstone reservoir, *ACS Omega* 8 (40) (2023) 37176–37185.
- [90] L. Zhang, H. Wang, F. Zhou, J. Mou, Numerical simulation of wormhole propagation with foamed-viscoelastic-surfactant acid in carbonate acidizing, *Processes* 11 (2023) 1839.
- [91] M. Mahmoud, Y. Al-Duailej, M. Al-Khaldi, NMR as a characterization tool for wormholes: the complete picture, Abu Dhabi, United Arab Emirates, in: Proceedings of the Abu Dhabi International Petroleum Exhibition and Conference, 2016 (SPE- 171699-MS).
- [92] N. Qi, B. Li, G. Chen, M. Fang, B. Li, C. Liang, X. Ren, K. Zhang, Damköhler number-based research on dividing dissolution patterns in carbonate acidizing, *J. Pet. Sci. Eng.* 170 (2018) 922–931.
- [93] F. Golfier, B. Bazin, R. Lenormand, M. Quintard, Core-scale description of porous media dissolution during acid injection - Part I: theoretical development, *Comput. Appl. Math.* 23 (2–3) (2004).
- [94] Ahmed M. Gomma, W. Guanqun, H.A. Nasr-El-Din, An experimental study of a new VES acid system: considering the impact of CO₂ solubility, The Woodlands, Texas, USA, in: SPE International Symposium on Oilfield Chemistry, April 2011 (SPE- 141298-MS).
- [95] H. Younesian-Farid, S. Sadeghnejad, Geochemical performance evaluation of pre-flushing of weak and strong acids during pH-triggered polymer flooding, *J. Pet. Sci. Eng.* 174 (2019) 1022–1033.
- [96] M.A.F. Rodrigues, G.M. Arruda, D.S. da Silva, F.M.F. da Costa, M.F.P. de Brito, A.C.D. Antonino, A.D.O. Wanderley Neto, Application of nonionic surfactant nonylphenol to control acid stimulation in carbonate matrix, *J. Pet. Sci. Eng.* 203 (2021) 108654.
- [97] G. Daccord, R. Lenormand, O. Lietard, Chemical dissolution of a porous medium by a reactive fluid-1. Model for the “wormholing” phenomenon, *Chem. Eng. Sci.* 48 (1993) 169.
- [98] B. Bazin, C. Roque, M. Bouteica, A laboratory evaluation of acid propagation in relation to acid fracturing: results and interpretation, The Hague, Netherlands, in: European Formation Damage Conference, 1995. SPE-30085.
- [99] M. Ziauddin, E. Bize, The effect of pore-scale heterogeneities on carbonate stimulation treatments, Kingdom of Bahrain, in: SPE Middle East Oil and Gas Show and Conference, 2007. SPE-104627.
- [100] M.S. Talbot, R.D. Gdanski, Beyond the damkohler number: a new interpretation of carbonate wormholing, in: SPE Europe/EAGE Annual Conference and Exhibition, 2008. SPE-113042.